Windhoekite, $Ca_2Fe^{3+}_{3-x}(Si_8O_{20})(OH)_4 \cdot 10H_2O$, a new palygorskite-group mineral from the Aris phonolite, Namibia

NIKITA V. CHUKANOV[1,*], SERGEY N. BRITVIN[2,3], GÜNTER BLASS[4], DMITRIY I. BELAKOVSKIY[5]
and KONSTANTIN V. VAN[6]

[1] Institute of Problems of Chemical Physics, Russian Academy of Sciences, Chernogolovka,
Moscow region 142432, Russia
*Corresponding author, e-mail: chukanov@icp.ac.ru
[2] Department of Crystallography, St. Petersburg State University, Universitetskaya Nab. 7/9,
St Petersburg 199034, Russia
[3] Nanomaterials Research Center, Kola Science Center, Russian Academy of Sciences, 184200 Apatity,
Murmansk Region, Russia
[4] Merzbachstrasse 6, 52249 Eschweiler, Germany
[5] Fersman Mineralogical Museum of the Russian Academy of Sciences, Leninsky Prospekt 8-2,
Moscow, 117071, Russia
[6] Institute of Experimental Mineralogy, Russian Academy of Sciences, Chernogolovka, Moscow Region 142432, Russia

Abstract: The new mineral windhoekite was discovered in a specimen from the Ariskop Quarry, near Windhoek, Namibia. Associated minerals are fluorapophyllite, aegirine, microcline, arisite-(Ce), arisite-(La). Windhoekite is yellow-brown, translucent; streak is beige. It forms isolated long-prismatic crystals up to 0.15×4 mm and their radial aggregates in cavities in phonolite. D_{calc} is 2.630 g/cm^3, D_{meas} is 2.62 (2) g/cm^3. The new mineral is biaxial (-), $\alpha = 1.610(3)$, $\beta = 1.662(3)$, $\gamma = 1.671(3)$, 2V (meas.) = 50(10)°, 2V (calc.) = 44°. Dispersion is not observed, pleochroism is strong ($Y \approx Z > X$, brown to dark brown), orientation: $X \approx a$; $Z = c$. The IR spectrum is given. The chemical composition is (electron microprobe, mean of 5 analyses, wt%): CaO 9.24, MnO 0.85, Fe_2O_3 23.14, Al_2O_3 0.41, SiO_2 46.32, H_2O (by gas chromatography) 21.0; total 100.96. The empirical formula based on 34 O atoms is: $(Ca_{1.68}Mn_{0.12})Fe^{3+}_{2.96}(Si_{7.87}Al_{0.08}O_{20})(OH)_4 \cdot 10H_{1.98}O$. The simplified formula is: $Ca_2Fe^{3+}_{3-x}[(Si,Al)_8O_{20}](OH)_4 \cdot 10H_2O$. The crystal structure was solved using single-crystal diffraction data. Windhoekite is monoclinic, space group $C2/m$, $a = 14.319(5)$, $b = 17.825(4)$, $c = 5.242(1)$ Å, $\beta = 103.5(2)°$, $V = 1301.0(6)$ Å^3, $Z = 2$. Ca and Fe^{3+} occupy two large octahedra and two smaller octahedra, respectively. The strongest lines of the powder diffraction pattern [d, Å (I, %) (hkl)] are: 11.04 (100) (110), 4.432 (10) (021), 4.133 (6) (22-1), 3.754 (4) (240), 3.486 (11) (400), 2.636 (8) (35-1), 2.551 (4) (002), 2.505 (6) (26-1). Type material is deposited in the collections of the Fersman Mineralogical Museum of the Russian Academy of Sciences, Moscow, Russia, under registration number 4018/1.

Key-words: windhoekite, new mineral, palygorskite group, crystal structure, Aris, Namibia.

1. Introduction

The Aris phonolite intrusion in southwestern Namibia is a well-known occurrence of alkaline mineral assemblages. Sodium-rich Fe- and Mn- minerals related to the palygorskite group are quite common at the Aris intrusion (Cámara *et al.*, 2002). Wide variations of chemical composition along with availability of relatively good crystals prompted us to a further systematic study of the palygorskite-group minerals originating from this intrusion. As a result of microprobe studies, a series of minerals related to palygorskite have been identified, including a number of Ca-rich samples (Table 1). Further detailed investigations demonstrated that the latter are a new mineral species, namely the Ca-Fe-dominant member of the palygorskite group. It was named windhoekite, for the type locality at the Aris intrusion in the Windhoek district, Namibia. The mineral and the name have been approved by the IMA Commission on New Minerals, Nomenclature and Classification (IMA no. 2010-083). The type material is deposited in the collection of the Fersman Mineralogical Museum of the Russian Academy of Sciences, Moscow, Russia, registration number 4018/1.

Table 1. Analytical results for windhoekite and related minerals from the Aris phonolite.

	Sample						Probe standard
	1	2	3	4	5	6	
Wt%							
K_2O	*bdl*	0.34	*bdl*	0.08	*bdl*	*bdl*	Microcline
Na_2O	*bdl*	1.16	0.18	0.83	6.34	6.56	Albite
CaO	9.24 (9.00–9.58)	5.80	6.39	1.62	*bdl*	*bdl*	Wollastonite
MgO	*bdl*	0.12	3.59	20.33	*bdl*	*bdl*	Diopside
MnO	0.85 (0.63–1.06)	2.63	2.91	1.21	2.32	9.01	$MnTiO_3$
Fe_2O_3[a]	23.14 (22.03–24.01)	25.17	19.70	3.81	21.33	9.36	Fe_2O_3
Cr_2O_3	*bdl*	0.32	*bdl*	*bdl*	*bdl*	0.39	Cr
TiO_2	*bdl*	0.73	*bdl*	0.99	0.56	3.41	TiO_2
Al_2O_3	0.41 (0.24–0.70)	2.57	0.95	2.13	0.84	0.46	Al_2O_3
SiO_2	46.32 (45.94–46.61)	40.04	48.94	50.99	46.61	50.65	SiO_2
H_2O	21.0	*nd*	*nd*	*nd*	*nd*	*nd*	
Total	100.96	78.88	82.66	81.99	78.00	79.84	
			Atoms per formula unit				
K	–	0.08	–	0.02	–	–	
Na	–	0.42	0.06	0.24	2.07	1.99	
Ca	1.62	1.15	1.09	0.24	–	–	
Mg	–	0.04	0.85	4.53	–	–	
Mn	0.12	0.41	0.40	0.15	0.33	1.20	
Fe	2.96	3.52	2.37	0.43	2.70	1.10	
Cr	–	0.04	–	–	–	0.05	
Ti	–	0.10	–	0.11	0.07	0.40	
Al	0.08	0.56	0.18	0.38	0.16	0.08	
Si	7.87	7.44	7.82	7.62	7.84	7.92	
H	19.8	–	–	–	–	–	

1 – windhoekite holotype (ranges are given in parenthesis); 2 – windhoekite, Na-rich variety; 3 – windhoekite, Mg-rich variety; 4 – palygorskite forming epitaxy on Mg-bearing windhoekite; 5 – tuperssuatsiaite; 6 – Mn-rich mineral forming epitaxy on tuperssuatsiaite. Basis of calculation of formula coefficients: 34 O atoms for windhoekite holotype and $(Si,Al)_8$ for other samples.
bdl, below detection limit; *nd*, not determined.
[a]Taking into account the values of Fe-O distances in octahedra occupied by Fe, all iron in windhoekite is considered to be trivalent.

2. Occurrence, general appearance and physical properties

Specimens with windhoekite, tuperssuatsiaite and other minerals related to palygorskite have been collected on the dumps of the Ariskop Quarry, Aris, near Windhoek, Windhoek district, Khomas Region, Namibia. All these minerals occur in miarolitic cavities of phonolite and, like the majority of late minerals from this locality, are related to the hydrothermal stage of phonolite formation. Associated minerals are fluorapophyllite, aegirine, microcline and arisite whose crystals contain Ce- and La-dominant zones. The order of mineral formation is as follows: microcline → aegirine → fluorapophyllite → palygorskite-group minerals + arisite.

Minerals related to palygorskite are visually indistinguishable. They form isolated long-prismatic to acicular isolated crystals and their radiated and random aggregates. The colour varies from brownish-yellow to green. By chemical composition, most of them correspond to tuperssuatsiaite (see analysis 5 in Table 1). Rarely outer zones (several μm thick) of acicular tuperssuatsiaite crystals are Mn-dominant (with Mn > Fe in atomic proportions) and enriched in Ti. One cannot exclude that these zones correspond to raite.

Na-poor minerals related to palygorskite are rare. In particular, windhoekite, the new Ca-dominant palygorskite-group mineral, is known in three specimens and consequently is represented by three compositional varieties (Fig. 1–3; analyses 1–3 in Table 1). Crystals of an Mg-rich
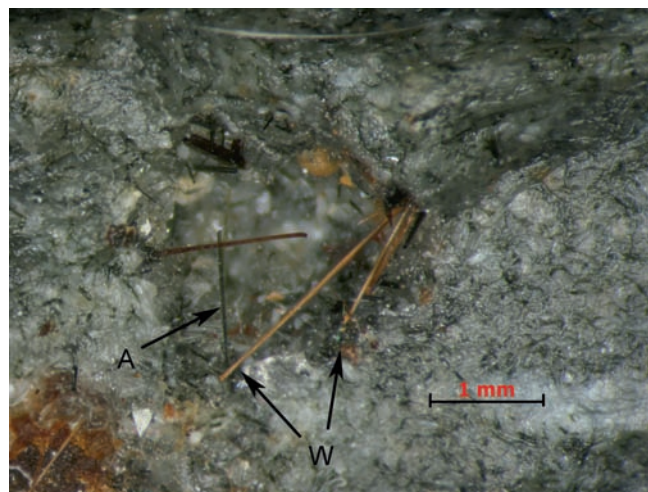

Fig. 1. Crystals of holotype windhoekite (W) with aegirine (A).

Fig. 2. Radial aggregates of windhoekite.

Fig. 3. Cluster of windhoekite crystals capped by epitaxial overgrowths of palygorskite (light ends of crystals).

variety of windhoekite are capped by epitaxial overgrowths of palygorskite (analysis 4 in Table 1).

Aegirine from the association with windhoekite is characterized by low contents of Ca. Its empirical formula is $(Na_{0.93}Ca_{0.04})(Fe_{0.89}Al_{0.03}Mg_{0.05}Ti_{0.03})Si_2O_6$. Note that strong enhancement of the activity of Ca during the latest hydrothermal stages of evolution of peralkaline complexes (along with the lowering of Na activity) is a well-known phenomenon (Lovskaya *et al.*, 2002; Moiseev & Chukanov, 2006) whose mechanism is not fully understood.

Windhoekite forms isolated long-prismatic crystals, up to 0.15 mm across and 4 mm in length, and their radial aggregates up to 5 mm in size on the walls of cavities in a phonolite (Fig. 1 and 2). Windhoekite is translucent, brown to yellowish-brown, with vitreous or silky lustre. The powder colour is beige. Windhoekite is sectile, Mohs hardness is 2. It shows perfect cleavage on (100). Density measured by flotation in heavy liquids is 2.62(2) g/cm³. Calculated density is 2.630 g/cm³. Optically, the new mineral is biaxial (-), $\alpha = 1.610(3)$, $\beta = 1.662(3)$,
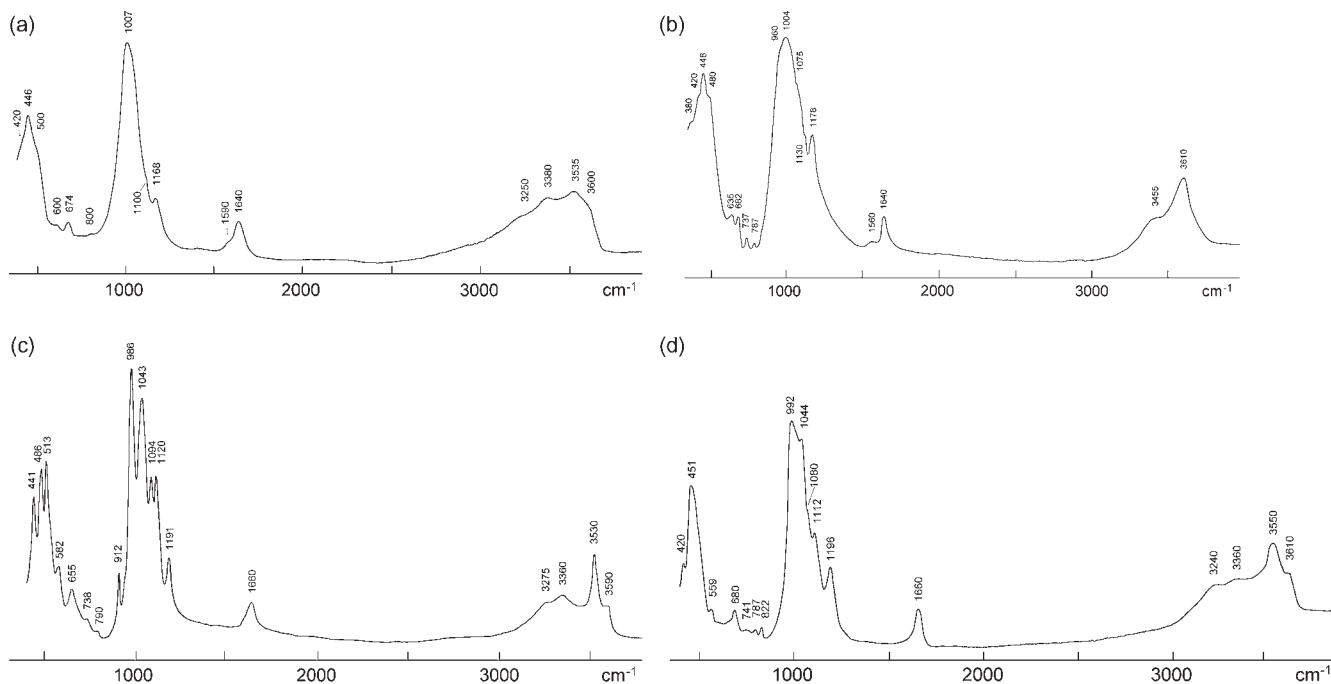

Fig. 4. Infrared spectra of palygorskite-group minerals: windhoekite (a), tuperssuatsiaite from Aris, Namibia (b), palygorskite from Penchi, China (c), and yofortierite from Mt. Karnasurt, Lovozero massif, Kola peninsula, Russia (d).

Table 2. Crystal parameters, data collection and structure refinement details for the twinned crystal of windhoekite.

Crystal data	
Formula	$(Ca_{1.69}Mn^{2+}_{0.21})_{1.90}Fe^{3+}_{2.66}[Si_{7.91}Al_{0.09}O_{18.31}(OH)_{1.69}](OH)_{2.00} \cdot 8.16H_2O$
Simplified formula	$Ca_{2-x}Fe^{3+}_{3-y}[Si_8O_{20}](OH)_2 \cdot 10H_2O^a$
Crystal size (mm)	$0.46 \times 0.06 \times 0.05$
Crystal system	Monoclinic
Space group	$C2/m$
a (Å)	14.319(5)
b (Å)	17.825(4)
c (Å)	5.242(1)
β (degrees)	103.5(2)
V (Å^3)	1,301.0(6)
Z	2
D_x (g/cm^3)	2.46
Data collection	
Instrument	Stoe IPDS II (image plate detector)
Radiation	Mo$K\alpha$ ($\lambda = 0.71073$ Å)
Average temperature (K)	293
Detector to sample distance (mm)	80
Omega increment (degrees)	2
Number of frames	90
Exposure per frame (min)	5
2Θ range (degrees)	2.86–64.80
Total collected reflections	10,117
Unique reflections	4,064
Unique observed $|F_o| \geq 4\sigma_F$	2,966
$R_{int.}$	0.099
R_σ	0.035
hkl range	$-16 \leq h \leq 16; -20 \leq k \leq 20; -5 \leq l \leq 6$
Refinement	
Reflection file type	HKLF 5
Twin matrix	$[-1\ 0\ -1][0\ -1\ 0]\ [0\ 0\ 1]$
R_1 ($|F_o| \geq 4\sigma_F$)	0.131
R_1 (all data)	0.154
wR_2	0.386
$S = GooF$	1.483

^{a}The water content in simplified formula is given based on direct chromatographic determination.

$\gamma = 1.671(3)$. 2V (meas.) = 50(10)°, 2V (calc.) = 44°. Dispersion is not observed. Orientation: $X \approx a$; $Z = c$. Pleochroism is strong, $Y \approx Z > X$ (brown to dark brown).

3. Chemical data

Electron-microprobe analyses were carried out using a VEGA TS 5130MM scanning electron microscope (SEM) equipped with energy-dispersive X-ray analyser (EDX, with INCA Si(Li) detector), at an operating voltage of 15.7 kV and a beam current of 0.5 nA. The electron beam was rastered over an area 16×16 μm^2. The H$_2$O content was determined by gas chromatography of the products of annealing at 1200 °C. CO$_2$ was not analysed because of the absence of bands corresponding to vibrations of C-O bonds in the IR spectrum. The contents of F, Na, Mg, P, S, Cl, K, Ti, and Cr were found to be below detection limits. Analytical results are given in Table 1. The empirical formula of windhoekite (based on 34 O atoms) is: $(Ca_{1.68}Mn_{0.12})Fe^{3+}_{2.96}(Si_{7.87}Al_{0.08}O_{20})(OH)_4 \cdot 10H_{1.98}O$. The simplified formula, taking into account structural data (see below), can be expressed as $Ca_2Fe^{3+}_{3-x}[(Si,Al)_8O_{20}](OH)_4 \cdot 10H_2O$. The idealized formula, $Ca_2Fe^{3+}_{2.67}(Si_8O_{20})(OH)_4 \cdot 10H_2O$, requires CaO 10.97, Fe$_2O_3$ 20.86, SiO$_2$ 47.03, H$_2$O 21.15, total 100.01 wt%. The Gladstone-Dale compatibility index calculated from the empirical formula is 1 - (K_P/K_c) = 0.012 (superior).

4. Infrared spectroscopy

Windhoekite powder was mixed with anhydrous KBr, pelletized, and analysed using a Specord 75 IR spectrophotometer. The IR spectrum of a pure KBr-disk was subtracted from the overall spectrum. Polystyrene and gaseous NH$_3$ were used as frequency standards; the precision of frequency measurement is ± 1 cm^{-1}; the mean resolution for the range 400–1600 cm^{-1} is 0.8 cm^{-1}.

The IR spectrum of windhoekite differs from those of other palygorskite-group minerals (Fig. 4). Absorption

Table 3. Bond valence calculations for Fe sites $M1$ and $M2$ in the structure of windhoekite.

Central atom	Ligand	Distance (Å)	Occupancy	Formal charge	Mean bond length (Å)
Fe1	O1	2.067×4	1.00	1.74	
Fe1	O4	1.933×2		1.25	
				2.99	2.022
Fe2	O1	2.089×2	0.88	0.93	
Fe2	O2	2.023×2		1.11	
Fe2	O4	2.054×2		1.02	
				3.07	2.055

Table 4. Fractional atomic coordinates, isotropic displacement parameters (Å^2) and site occupancies in the crystal structure of windhoekite.

Site	x	y	z	U_{iso}	Occupancy
Si1	0.3001 (1)	0.4162 (1)	0.0314 (5)	0.0222 (6)	1
Si2	0.2987 (1)	0.3313 (1)	0.5262 (5)	0.0272 (6)	1
M1	1/2	1/2	0	0.0294 (7)	$Fe^{3+}_{1.00}$
M2	1/2	0.4126 (1)	1/2	0.0301 (8)	$Fe^{3+}_{0.88}$
M3	1/2	0.3130 (3)	0	0.057 (2)	$Ca_{0.62}Mn^{2+}_{0.04}$
M4	1/2	0.2300 (5)	1/2	0.053 (3)	$Ca_{0.37}Mn^{2+}_{0.03}$
O1	0.4180 (3)	0.4167 (3)	0.1144 (13)	0.026 (1)	1
O2	0.4154 (4)	0.3308 (3)	0.5910 (14)	0.036 (1)	1
O3	1/4	1/4	1/2	0.041 (2)	1
O4	0.5685 (5)	1/2	0.3644 (19)	0.033 (2)	1
O5	0.2576 (4)	1/2	0.0015 (17)	0.031 (2)	1
O6	0.2566 (3)	0.3735 (3)	0.2495 (10)	0.031 (2)	1
O7	0.2598 (3)	0.3745 (3)	0.755 (1)	0.032 (2)	1
OW1	0.106 (2)	1/2	0.361 (8)	0.26 (2)	1
OW2	0.4064 (9)	0.2302 (9)	0.107 (3)	0.132 (5)	1
OW3	0.487 (6)	0.106 (8)	0.698 (15)	0.87 (11)	1

Table 5. Anisotropic displacement parameters (Å^2) of atoms in the crystal structure of windhoekite.

| Site	U_{11}	U_{22}	U_{33}	U_{23}	U_{13}	U_{12}
Si1	0.045 (1)	0.010 (1)	0.016 (1)	−0.0011 (8)	0.015 (1)	−0.0034 (6)
Si2	0.053 (1)	0.010 (1)	0.024 (1)	−0.0001 (9)	0.020 (1)	−0.0030 (7)
M1	0.050 (1)	0.024 (1)	0.018 (1)	0	0.015 (1)	0
M2	0.051 (1)	0.023 (1)	0.022 (1)	0	0.019 (1)	0
M3	0.063 (3)	0.067 (4)	0.043 (3)	0	0.019 (2)	0
M4	0.065 (4)	0.045 (5)	0.050 (5)	0	0.016 (4)	0
O1	0.044 (3)	0.012 (3)	0.025 (3)	−0.002 (2)	0.016 (3)	−0.007 (2)
O2	0.052 (3)	0.023 (3)	0.037 (4)	−0.003 (3)	0.017 (3)	−0.001 (2)
O3	0.092 (5)	0.009 (4)	0.029 (5)	0.005 (3)	0.026 (4)	−0.017 (3)
O4	0.043 (4)	0.033 (5)	0.033 (5)	0	0.028 (4)	0
O5	0.057 (4)	0.008 (4)	0.031 (5)	0	0.019 (4)	0
O6	0.061 (3)	0.018 (3)	0.019 (4)	0.006 (2)	0.022 (2)	−0.001 (2)
O7	0.057 (3)	0.009 (3)	0.035 (5)	−0.006 (2)	0.023 (2)	−0.009 (2)
OW1	0.27 (3)	0.27 (5)	0.33 (5)	0	0.24 (3)	0
OW2	0.17 (1)	0.12 (1)	0.13 (1)	−0.01 (1)	0.083 (9)	0.019 (8)
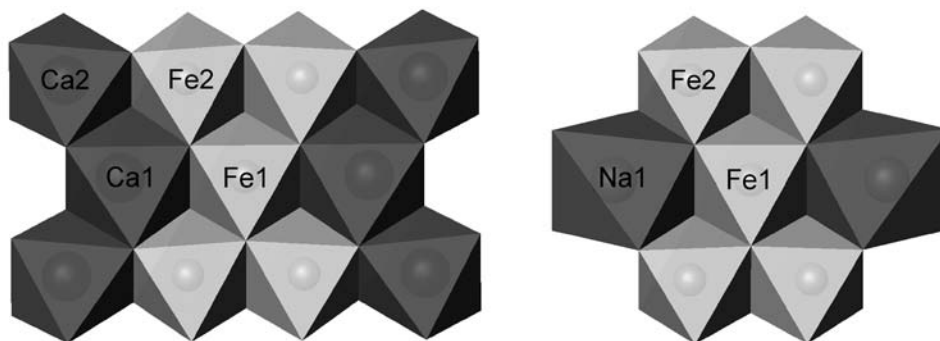
Fig. 5. Polyhedral representation of the crystal structures of windhoekite (left) and tuperssuatsiaite (right) projected on (001). Light grey octahedra correspond to Fe sites M1 and M2; dark grey octahedra correspond to Ca-dominant sites M3 and M4 in windhoekite and Na-dominant site in tuperssuatsiaite, respectively. Grey balls are H_2O molecules in the channels. The structure of tuperssuatsiaite is drawn based on the data by Cámara *et al.* (2002).

bands in the IR spectrum of windhoekite and their assignments (cm^{-1}; s – strong band, sh – shoulder) are: 3600 sh, 3535 s, 3380 s, 3250 sh (O–H stretching vibrations of H_2O molecules and OH groups); 1640, 1590 sh (bending vibrations of H_2O molecules); 1168 (stretching vibrations of Si–O–Si links with large Si-O-Si angles between
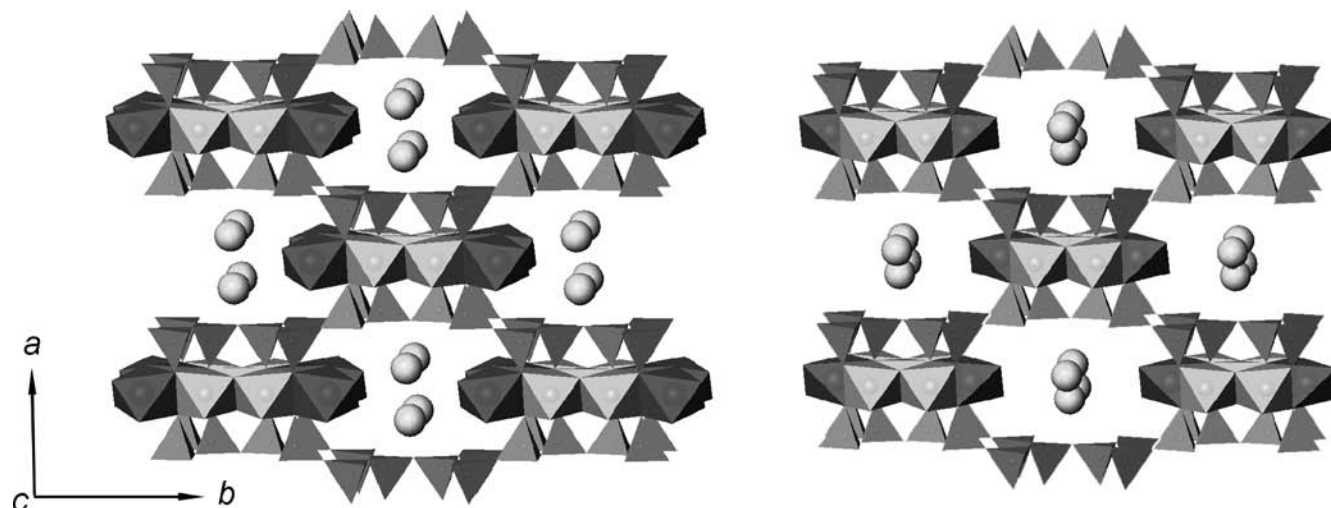
Fig. 6. Arrangement of octahedral sites in the crystal structures of windhoekite (left) and tuperssuatsiaite (right) projected on (100). An additional Ca2 (M4) site is present in the structure of windhoekite but missing in the structure of tuperssuatsiaite. Note that all outer corners of Ca1 and Ca2 octahedra in windhoekite are occupied by hydroxyl groups and water molecules (Fig. 6). The structure of tuperssuatsiaite is drawn based on the data by Cámara $et\ al$. (2002).
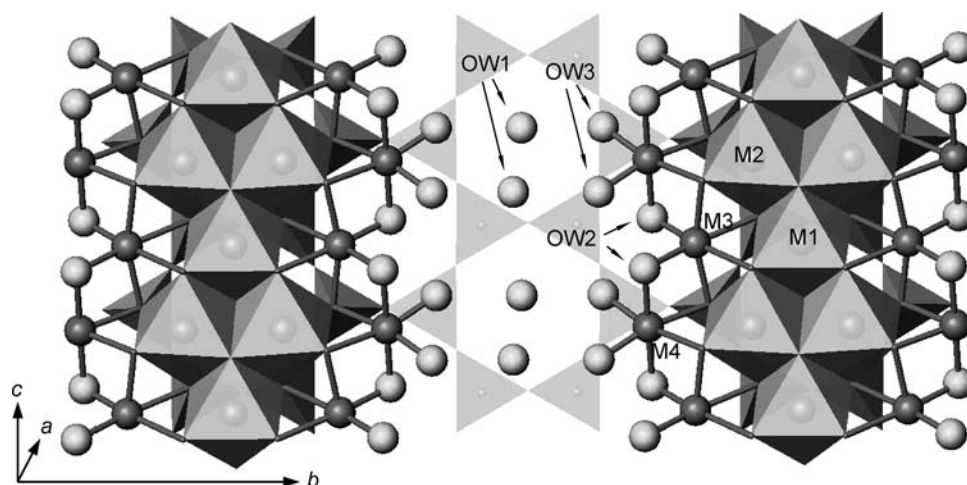

Fig. 7. Arrangement of intrachannel water molecules (OW1) and mixed (H_2O, OH) sites (OW2, OW3) in the crystal structure of windhoekite. The intrachannel-facing corners of Ca-dominant M3 and M4 octahedra are coordinated by water molecules and hydroxyls (OW2 and OW3).

neighbouring ribbons – see Tarte $et\ al$. (1973)); 1100 sh, 1007 s (Si–O stretching vibrations); 800, 674, 600 (Fe$\cdots$O–H bending vibrations and mixed vibrations of tetrahedral layers); 500 sh, 446 s, 420 sh (combination of Si–O–Si bending vibrations and stretching vibrations of FeO$_6$ octahedra). Bands of B- or C-bearing groups are absent.

The IR absorption bands of windhoekite are broad and badly resolved, which is in line with the disordering of cations (Ca, Fe^{3+}) and vacancies in the crystal structure. For this reason, the IR spectrum of windhoekite cannot be considered as its important diagnostic characteristic.

In the IR spectra palygorskite- and sepiolite-group minerals, the position of the band of stretching vibrations of Si–O–Si links between neighbouring ribbons can vary from 1150 to 1215 cm^{-1}. There are several factors influencing the position of this band. For example, in the

isomorphic series sepiolite-ferrosepiolite this band gradually shifts from 1212 to 1181 cm^{-1} with the growth of Fe content (Chukanova $et\ al$., 2002). In the course of acid leaching of palygorskite, the band near 1200 cm^{-1} shifts to lower wavenumbers (Cai $et\ al$., 2007). There are not so many silicate minerals giving IR bands in this range. Thus the presence of the band at 1168 cm^{-1} indicates the belonging of windhoekite to palysepioles.

5. Crystal structure and powder X-ray diffraction data

Single-crystal X-ray diffraction data for windhoekite were collected by means of a Stoe IPDS II diffractometer (image plate detector, graphite-monochromatized Mo$K\alpha$ radiation). Subsequent data processing was carried out with

Table 6. X-ray powder diffraction data for windhoekite.

$d_{obs.}$	$I_{obs.}$	$d_{calc.}$[a]	$I_{calc.}$[b]	h	k	l	$d_{obs.}$	$I_{obs.}$	$d_{calc.}$[a]	$I_{calc.}$[b]	h	k	l
11.04	100	10.98	100	1	1	0	2.193	3	2.193	4	4	6	−1
8.95	2	8.91	1	0	2	0			2.166	1	5	5	−1
7.02	2	6.97	3	2	0	0	2.132	2	2.134	1	3	7	−1
5.50	2	5.49	0.5	2	2	0			2.131	1	5	1	−2
		5.46	0.5	1	3	0	2.065	1	2.066	1	4	4	−2
5.08	2	5.10	1	0	0	1	1.963	1	1.967	1	3	7	1
		4.454	1	0	4	0			1.961	1	4	6	1
4.432	10	4.427	6	0	2	1			1.959	1	6	0	−2
		4.335	1	1	1	1			1.863	1	4	0	2
4.134	6	4.133	2	2	2	−1	1.836	1	1.833	1	6	6	−1
		3.827	1	3	1	−1	1.759	1	1.758	2	7	5	−1
3.749	4	3.754	5	2	4	0	1.690	1	1.689	1	5	1	2
		3.727	1	2	0	1	1.682	1	1.682	1	0	10	1
		3.661	2	3	3	0	1.609	1	1.609	2	1	11	0
3.486	11	3.487	11	4	0	0	1.559	2	1.562	1	1	5	−3
		3.438	2	2	2	1			1.558	1	3	5	−3
3.279	1	3.271	2	3	3	−1			1.553	1	7	5	1
3.058	2	3.054	2	4	2	−1			1.549	1	6	0	2
2.933	2	2.939	2	1	5	−1	1.530	1	1.527	1	8	6	−1
2.754	2	2.756	4	5	1	0	1.507	1	1.507	2	2	6	−3
		2.747	1	3	3	1	1.483	1					
2.636	8	2.636	9	3	5	−1	1.472	1					
		2.591	1	1	1	−2	1.381	1					
2.550	4	2.551	4	0	0	2	1.373	1					
2.507	6	2.505	8	2	6	−1	1.364	1					
2.393	2	2.391	3	1	1	2	1.347	1					
2.341	1	2.338	3	3	5	1	1.295	1					
		2.322	1	2	6	1	1.284	1					
2.238	2	2.235	2	2	0	2	1.268	1					
		2.214	1	0	4	2							

[a] Calculated from cell parameters refined from powder data.
[b] Calculated from structural data.

Stoe X-Area 2.08 software (Stoe & Cie GmbH, 2004). Numerical absorption correction has been applied to the reflection dataset that was used for further direct solution of the crystal structure and its refinement (*SHELX*-97). The details of data collection and structure refinement are given in Table 2. The results of bond-valence calculations for selected atoms, fractional atomic coordinates and displacement parameters are listed in Tables 3–5, respectively. The crystal structure of windhoekite (Fig. 5–7) is closely related to those of tuperssuatsiaite (Cámara *et al.*, 2002) and raite (Pluth *et al.*, 1997); these three minerals can be considered as end members of the *palysepiole* polysomatic series (Ferraris *et al.*, 2004) with crystal structures being derivatives of palygorskite (Chisholm, 1992; Post & Heaney, 2008) and sepiolite (Post *et al.*, 2007).

The structures of these minerals are based on a hetero-polyhedral quasi-framework formed by chessboard connected triple (*TOT*) ribbons that develop along [001]. Outer tetrahedral (*T*) parts of neighbouring ribbons are connected via common vertices to form crimped tetrahedral 2D sheets that are connected via inner (octahedral, *O*) parts of the ribbons. Octahedral parts of *TOT* ribbons are three octahedra wide in palygorskite-group minerals (palygorskite, yofortierite and tuperssuatsiaite) and four octahedra wide in the members of the sepiolite group (sepiolite, ferrosepiolite, falcondoite and loughlinite).

The octahedra have different cation-anion distances and can be occupied by Mg, Fe^{2+}, Ni, Al, Fe^{3+} and Na, whereas tetrahedra are predominantly occupied by Si. The structure of raite is based on a palygorskite-type framework. Kalifersite has a hybride structure between that of sepiolite and palygorskite, with alternating ribbons of the two types. Intersilite contains sepiolite-like ribbons that differ from sepiolite ones by inversions of tetrahedra. For palygorskite, two polytypes are known: monoclinic (*C*2/*m*) and orthorhombic (*Pbmn*) ones – Artioli & Galli (1994).

In all these minerals, heteropolyhedral quasi-frameworks contain [001] channels that are filled by highly disordered zeolitic H_2O molecules and can contain some low-force-strength exchange cations like Na, K or Ca.

For detailed review of the crystal chemistry of the *palysepiole* series, the reader is referred to Ferraris *et al.* (2004) and Ferraris & Gula (2005). From the chemical point of view, windhoekite is closely related to tuperssuatsiaite (Karup-Møller & Petersen, 1984; von Knorring *et al.*, 1992), the iron-dominant *palysepiole* mineral widely occurring in Aris phonolite (Cámara *et al.*, 2002). In the structures of both minerals, relatively small octahedral sites (*M*1 and *M*2) are predominantly occupied by Fe^{3+} while the larger octahedron *M*3 is occupied by Na in tuperssuatsiaite and, correspondingly, Ca in windhoekite.

Table 7. Comparative data for windhoekite and other palygorskite-group minerals.

Mineral	Windhoekite	Palygorskite[a]	Yofortierite	Tuperssuatsiaite
Formula	$Ca_2Fe^{3+}_{3-x}$ $[(Si,Al)_8O_{20}]$ $(OH)_4 \cdot 10H_2O$	$(Mg,Al)_4(Si_8O_{20})$ $(OH)_2 \cdot 8H_2O$	$Mn^{2+}_5(Si_8O_{20})$ $(OH)_2 \cdot 8–9H_2O$	$Na_{2-x}(Fe^{3+},Mn)_3$ $(Si_8O_{20})(OH)_2 \cdot 4H_2O$
Space group	$C2/m$	$C2/m$	Pn?	$C2/m$, $C2/c$ or Cc
a, Å	14.319	12.75–13.14	12.759	13.92–14.034
b, Å	17.825	17.85–18.06	18.369	17.70–17.841
c, Å	5.242	5.12–5.24	5.024	5.265–5.30
β, °	103.5	91.1–107.0	91.98	103.67–104.78
Z	2	2	2	2
Strong lines of the X-ray powder-diffraction pattern: d, Å (I, %)	11.04 (100) 4.432 (10) 4.134 (6) 3.486 (11) 2.636 (8) 2.507 (6)	10.44 (100) 4.466 (20) 4.262 (22) 3.679 (15) 3.096 (16) 2.539 (20)	10.5 (100) 4.41 (18) 3.68 (15) 3.302 (90) 2.621 (30) 2.526 (15) 2.510 (20)	10.82 (100) 4.14 (20) 3.395 (30) 2.638 (40) 2.544 (30) 2.510 (30) 2.235 (30)
Optical data:				
α	1.610	1.50–1.56	1.530	1.54
β	1.662	1.52–1.55	n. d.	1.56
γ	1.671	1.53–1.57	1.559	1.58–1.60
Optical sign, 2V	−50	−30 to −60	n. d.	n. d.
Density, g cm^{-3}	2.630 (calc.)	2.35 (calc.)	2.82 (calc.)	2.28 (calc.)
Strongest IR absorption bands, cm^{-1}	3535 3380 1640 1168 1007 674 446	3530 3360 1660 1191 1120 1094 1043 986 912 655 582 513 486 441	3550 3360 1660 1196 1112 1044 992 680 559 451 420	3610 3455 1640 1178 1004 682 635 480 448
References	This work	Chisholm (1992); Christ et al. (1969); Giustetto & Chiari (2004); Mineraly (1992); this work	Horváth et al. (1998); Perrault et al. (1975); Mineraly (1992); this work	Karup-Møller & Petersen (1984); von Knorring et al. (1992); Mineraly (1992); this work

[a]Monoclinic variety.

However, the crystal structure of windhoekite bears additional octahedral site (M4) partially occupied by Ca^{2+} and missing in the structure of tuperssuatsiaite (Fig. 6). The occurrence of this new site indicates high flexibility of palygorskite-like structures toward introduction of even quite large cations. Both sites occupied by Ca (M3 and M4) are partially coordinated by water molecules and hydroxyl groups located in the channels of the structure (Fig. 7). Displacement parameters for OW3 could not be refined anisotropically, and so OW3 was refined isotropically. Note that similarly large ($U_{iso} = 0.5$) displacement parameters have been found by Cámara et al. (2002) for intrachannel water in tuperssuatsiaite. While OW3 obviously represents intrachannel molecular H_2O, the very defect nature of OW2 and OW1 sites ''incrustating'' the walls of structural channels equally allows the

existence of H_2O molecules as well as OH$^-$ groups. The low occupancies of these sites suggest that any bond-valence calculations related to these oxygen atoms are of little applicability, in terms of chemical formula calculations. The difficulties and consequent uncertainties in refining the occupancies of OW1, OW2, and OW3 are the reasons for the inconsistency of the total amount of water determined by chemical methods and the water found during structure refinement. Therefore, when calculating the stoichiometry of windhoekite, namely H_2O/OH ratio, we have relied upon the data of chemical analyses and charge-balance considerations rather than bond-valence calculations from structure refinement. Large displacement parameters for OW1, OW2 and OW3 indicate high degree of disorder of water molecules situated in (or at the walls of) the channels. However, one cannot rule out

that this can be partially accounted for by the poor quality of the crystal used for data collection and structure solution. The poor quality of crystals of the *palysepiole* series minerals is the main reason limiting the number of their crystal structures solved to date.

Powder X-ray diffraction data for windhoekite were collected using a Stoe IPDS II image plate diffractometer (Gandolfi geometry) using Mo$K\alpha$ radiation and are given in Table 6. They are well indexed in the monoclinic unit cell found by single-crystal studies; the refined unit-cell parameters are: $a = 14.339(9)$, $b = 17.817(4)$, $c = 5.245(3)$ Å, $\beta = 103.4(7)°$, $V = 1303(2)$ Å^3 (Table 7).

6. Discussion and conclusion

Due to the natural diversity of minerals related to the *palysepiole* polysomatic series (Ferraris *et al.*, 2004; Ferraris & Gula, 2005), their crystal chemistry attracts considerable scientific interest (Perrault *et al.*, 1975; Pluth *et al.*, 1997; Cámara *et al.*, 2002; Post *et al.*, 2007; Post & Heaney, 2008). However, due to experimental difficulties related to the poor crystal quality of these minerals, the number of their crystal structures solved and refined by single-crystal methods is still rather scarce. In this respect, the structural study of a new representative of the palysepiole series could be considered as an interesting contribution to the crystal chemistry of palysepiole minerals. The occurrence of a new octahedral site in the palygorskite-related structure might help in further understanding of mechanisms involved in chemical variations of these scientifically and industrially important compounds.

References

Artioli, G. & Galli, E. (1994): The crystal structures of orthorhombic and monoclinic palygorskite. *Mater. Sci. Forum.*, **166–169**, 647–652.

Cai, Y., Xue, J., Polya, D.A. (2007): A Fourier transform infrared spectroscopic study of Mg-rich, Mg-poor and acid leached palygorskites. *Spectrochim. Acta A.*, **66**, **2**, 282–288.

Cámara, F., Garvie, L.A.J., Devouard, B., Groy, T.L., Buseck, P.R. (2002): The structure of Mn-rich tuperssuatsiaite: a palygorskite-related mineral. *Am. Mineral.*, **87**, 1458–1463.

Chisholm, J.E. (1992): Powder-diffraction patterns and structural models for palygorskite. *Can. Mineral.*, **30**, 61–73.

Christ, C.L., Hathaway, J.C., Hostetler, P.B., Shepard, A.O. (1969): Palygorskite: new X-ray data. *Am. Mineral.*, **54**, 198–205.

Chukanova, V.N., Pekov, I.V., Chukanov, N.V., Zadov, A.E. (2002): Iron-rich analogue of sepiolite and the conditions of its formation in the contact aureole of the Lovozero Alkaline Massif. *Geochem. Int.*, **40**, **12**, 1225–1229.

Ferraris, G. & Gula, A. (2005): Polysomatic aspects of microporous minerals – heterophyllosilicates, palysepioles and rhodesite-related structures. *Microporous Mesoporous Miner. Phases. Rev. Mineral. Geochem.*, **57**, 69–104.

Ferraris, G., Makovicky, E., Merlino, S. (2004): Crystallography of Modular Materials. *IUCr Monographs on Crystallography*, **15**, Oxford University Press, Oxford.

Giustetto, R. & Chiari, G. (2004): Crystal structure refinement of palygorskite from neutron powder diffraction. *Eur. J. Mineral.*, **16**, 521–532.

Horváth, L., Pfenninger-Horváth, E., Gault, R.A., Tarassoff, P. (1998): Mineralogy of the Saint-Amable sill, Varennes and Saint-Amable, Québec. *Mineral. Rec.*, **29**, 83–118.

Karup-Møller, S. & Petersen, O.V. (1984): Tuperssuatsiaite, a new mineral species from the Ilímaussaq intrusion in South Greenland. *Neues Jahrb. Mineral. Monatsh.*, **1984**, 501–512.

Lovskaya, E.V., Pekov, I.V., Kononkova, N.N., Turchkova, A.G. (2002): Mineralogy, geochemistry and origin of high-calcium hydrothermalites in Khibiny massif, Kola peninsula. *Zapiski Rossiiskogo Mineral. Obshchestva*, **131**, **2**, 17–29 (in Russian).

Mineraly (1992): Volume IV (2). Nauka, Moscow, 662 p; (in Russian).

Moiseev, M.M. & Chukanov, N.V. (2006): Mineralogy of alkaline pegmatites and hydrothermalites of the Kovdor massif. *New Data Miner.*, **41**, 56–70.

Perrault, G., Harwey, Y., Pertsowsky, R. (1975): La yofortierite, un nouveau silicate hydrate de manganèse de St-Hilaire, P.Q. *Can. Mineral.*, **13**, 68–74.

Pluth, J.J., Smith, J.V., Pushcharovsky, D.Y., Semenov, E.I., Bram, A., Riekel, C., Weber, H.P., Broach, R.W. (1997): Third-generation synchrotron x-ray diffraction of 6-μm crystal of raite, approximate to Na$_3$Mn$_3$Ti$_{0.25}$Si$_8$O$_{20}$(OH)$_2$·10H$_2$O, opens up new chemistry and physics of low-temperature minerals. *Proc. Nat. Acad. Sci. U.SA*, **94**, 12263–12267.

Post, J.E. & Heaney, P.J. (2008): Synchrotron powder X-ray diffraction study of the structure and dehydration behavior of palygorskite. *Am. Mineral.*, **93**, 667–675.

Post, J.E., Bish, D.L., Heaney, P.J. (2007): Synchrotron powder X-ray diffraction study of the structure and dehydration behavior of sepiolite. *Am. Mineral.*, **92**, 91–97.

Tarte, P., Pottier, M.J., Procès, A.M. (1973): Vibrational studies of silicates and germanates – V. IR and Raman spectra of pyrosilicates and pyrogermanates with a linear bridge. *Spectrochim. Acta*, **29A**, 1017–1027.

von Knorring, O., Petersen, O.V., Karup-Møller, S., Leonardsen, E.S., Condliffe, E. (1992): Tuperssuatsiaite from the Aris phonolite, Windhoek, Namibia. *Neues Jahrb. Mineral. Monatsh.*, **1992**, 145–152.